Accepted Manuscript

TETRAHYDROPROTOBERBERINE ALKALOIDS WITH DOPAMINE AND σ RECEPTOR AFFINITY
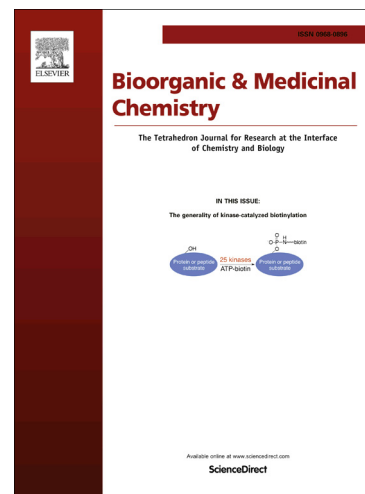
Satishkumar Gadhiya, Sudharshan Madapa, Thomas Kurtzman, Ian L. Alberts, Steven Ramsey, Nagavara-Kishore Pillarsetty, Teja Kalidindi, Wayne W. Harding

TETRAHYDROPROTOBERBERINE ALKALOIDS WITH DOPAMINE AND σ RECEPTOR AFFINITY

Satishkumar Gadhiya,[a,b] Sudharshan Madapa,[a] Thomas Kurtzman,[b,c,d] Ian L. Alberts,[e] Steven Ramsey,[c,d] Nagavara-Kishore Pillarsetty,[f] Teja Kalidindi[f] and Wayne W. Harding *,[a,b,c]

a. *Department of Chemistry, Hunter College, City University of New York, 695 Park Avenue, NY 10065, USA*

b. *Ph.D. Program in Chemistry, CUNY Graduate Center 365 5th Avenue, New York New York, United States of America, 10016*

c. *Ph.D. Program in Biochemistry, CUNY Graduate Center 365 5th Avenue, New York New York, United States of America, 10016*

d. *Department of Chemistry, Lehman College, The City University of New York, Bronx, NY 10468, USA.*

e. *Department of Natural Sciences, LaGuardia Community College, City University of New York, New York, NY 11101, USA*

f. *Department of Radiology, Memorial Sloan Kettering Cancer Center , 1275 York Avenue, New York, NY 10065, USA*

*Email: whardi@hunter.cuny.edu

*Tel: (+)212-772-5359*

Fax:(+)212-772-5332

ABSTRACT

Two series of analogues of the tetrahydroprotoberberine (THPB) alkaloid (±)-stepholidine that a) contain various alkoxy substituents at the C10 position and, b) were de-rigidified with respect to (±)-stepholidine, were synthesized and evaluated for affinity at dopamine and σ receptors in order to evaluate effects on D3 and σ2 receptor affinity and selectivity. Small *n*-alkoxy groups are best tolerated by D3 and σ2 receptors. Among all compounds tested, C10 methoxy and ethoxy analogues (**10** and **11** respectively) displayed the highest affinity for σ2 receptors as well as σ2 versus σ1 selectivity and also showed the highest D3 receptor affinity. De-rigidification of stepholidine resulted in decreased affinity at all receptors evaluated; thus the tetracyclic THPB framework is advantageous for affinity at dopamine and σ receptors. Docking of the C10 analogues at the D3 receptor, suggest that an ionic interaction between the protonated nitrogen atom and Asp110, a H-bond interaction between the C2 phenol and Ser192, a H-bond interaction between the C10 phenol and Cys181 as well as hydrophobic interactions of the aryl rings to Phe106 and Phe345, are critical for high affinity of the compounds.

GRAPHICAL ABSTRACT

Stepholidine
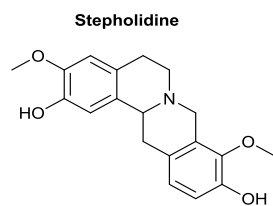
Ki at D3 = 101 nM
Ki at sigma-2 = 9 nM
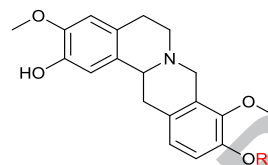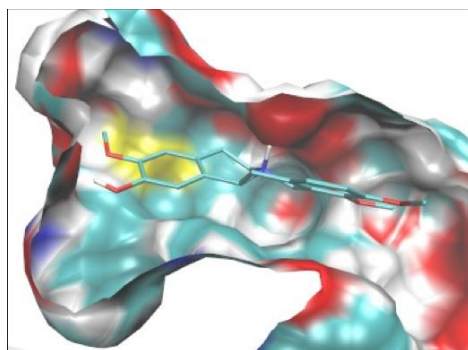
Ki at D3 = 37 - 220 nM
Ki at sigma-2 = 1 - 107 nM

1. Introduction

The dopamine D3 receptor has received considerable attention, especially over the past two decades, mainly due to its prominent role in mediating craving for addictive substances.[1-3] In that regard, selective D3 antagonists have been sought after as potential therapeutics for cocaine addiction and the treatment of cocaine relapse.[4] Additionally, a growing body of evidence in the literature suggests that D3 antagonism may be a valuable antipsychotic therapeutic strategy.[5-7] Several selective D3 antagonists have been identified that bear the key pharmacophoric elements of a phenylpiperazine motif connected to an aryl amide unit via a 4 carbon spacer.[8,9,1] Other D3-preferring scaffolds are also known, although the phenypiperazine template has been most prolific in terms of the number of compounds reported. Representative examples of selective D3 antagonists are depicted in Figure 1.
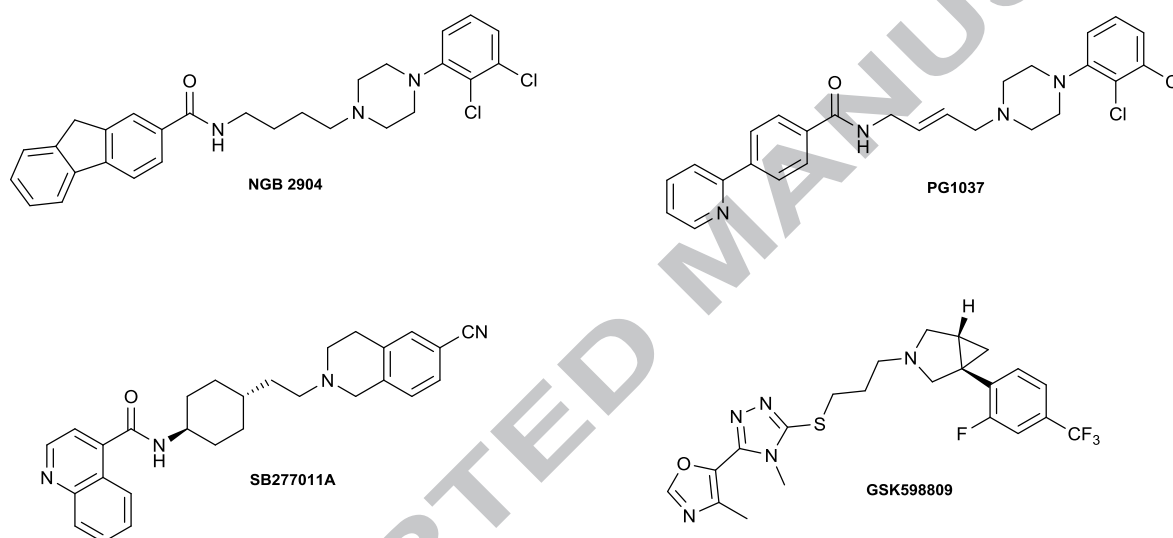
Figure 1. Structures of representative selective D3 antagonists

Despite advances in understanding the structure-activity relationships (SARs) of such D3 scaffolds, in most cases, clinical translation of the resulting optimized compounds has been limited, primarily due to pharmacokinetic issues.[3] There is thus a constant search for new structural templates endowed with selective D3 antagonist activity as such compounds could serve as useful leads for development as *in vivo* biological tools and therapeutic leads, especially pertinent to the realms of neuropsychiatric disorders and drug abuse.

There are two types of σ receptors - σ1 and σ2, as borne out by differential binding of selective radioligands as well as other biochemical and pharmacological studies.[10-12] σ receptors are distributed in the central nervous system (CNS) and in peripheral tissue.[13,14] Within the CNS, σ1 receptors are concentrated in the hippocampus and other limbic regions which control cognition and emotion.[15,16] Thus these receptors have been implicated in a number of neuropsychiatric disorders and have been targets for the development of treatment interventions for such diseases.[17-20] σ2 receptors are found predominantly in regions responsible for

4

motor functions in the CNS and are also highly expressed in the lung, liver and kidneys.[15,16] The σ1 receptor has been cloned but the σ2 receptor has not, and there is some debate about the identity of the σ2 receptor.[21] Recent studies suggest that the σ2 receptor is Progesterone Receptor Membrane Component 1 (PGRMC1).[22,23]
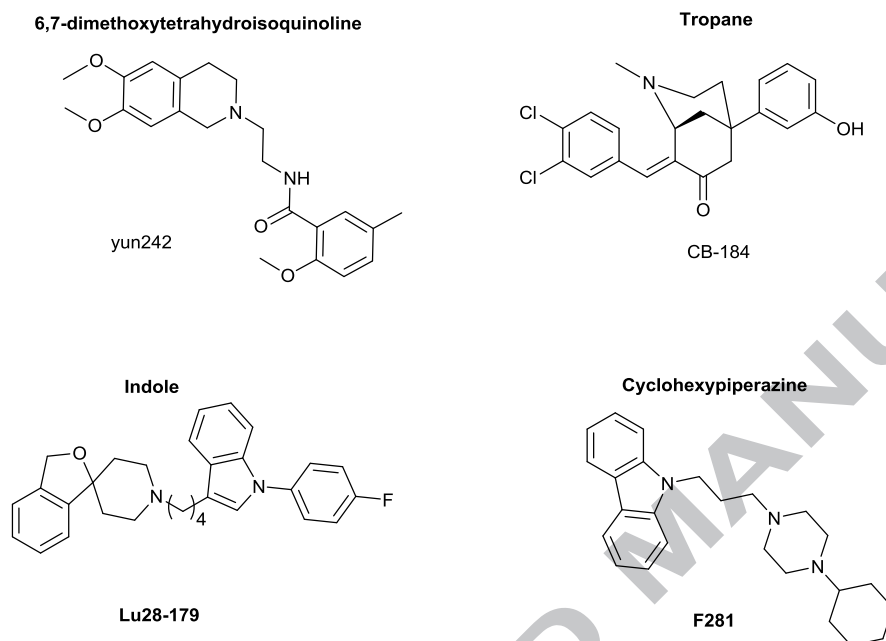

Figure 2. Structural classes of σ2ligands and representative examples

σ2 receptors are overexpressed in tumor cells and are upregulated in rapidly proliferating cells and this receptor has attracted interest as a biomarker for cancer proliferation.[24,25] Some σ2 ligands (particularly σ2 receptor agonists) display cytotoxic activity.[26] Thus, σ2 ligands have been of interest for the development of "stand alone" antitumor drugs, targeted drug delivery agents and Positron Emission Tomography (PET) tools for imaging the proliferative status of various cancers.[27-30] σ2 receptor ligands have been predominantly from four structural classes: 6,7-dimethoxytetrahydroisoquinolines, indoles, tropanes and cyclohexylpiperazines (Figure 2). Many of these compounds lack sufficient selectivity or are otherwise hampered by unfavorable pharmacokinetic drawbacks that limit their usefulness as drugs, anticancer drug delivery vehicles or tools. New, potent and selective σ2 receptor ligands are sought after to fully exploit the potential of the σ2 receptor as a target for cancer diagnosis and therapy.

The tetrahydroprotoberberine (THPB) alkaloid (-)-stepholidine (**1,** Figure 3) shows affinity for dopamine D1 and D2 receptors and has been the focus of a number of structure-activity relationship (SAR) studies in this regard.[31,32] The antipsychotic and anti-drug abuse potential of (-)-stepholidine has been attributed to its unusual D1 agonist/D2 antagonist profile. (-)-Stepholidine also shows good affinity for σ2 (K_i = 54 nM) and D3 receptors (K_i = 30 nM), as revealed by data from the Psychoactive Drug Screening Program (PDSP)

database.[33] Given the comparatively high σ2 and D3 affinity of **1**, we considered that the THPB template may be exploitable towards the development of novel potent and selective σ2 receptor or D3 receptor ligands. However, no SAR studies have been performed on THPBs in relation to their σ2 or D3 receptor affinity. Furthermore, computational evaluations on THPBs particularly at the D3 receptor (for which a crystal structure is available)[34] are lacking in the literature. Such studies could propel our understanding of the potential utility of this scaffold towards obtaining novel, selective σ2 or D3 receptor ligands. Our explorations in this regard are described herein.
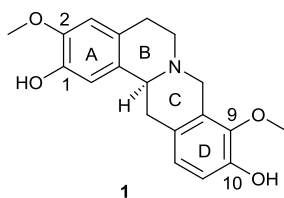

Figure 3. Structure of (-)-stepholidine (**1**)

2. Results and discussion

Stepholidine was used as the lead molecule for our SAR evaluations. To initiate this study, we decided to prepare a series of racemic C10 stepholidine analogues in order to probe the tolerance of this position for larger substituent groups at both receptors. THPBs are structurally similar to the 6,7-dimethoxytetrahydroisoquinoline class of σ2 ligands in that both possess a tetrahydroisoquinoline motif. Tetrahydroisoquinoline sub-structures are also found in a number of D3 antagonist ligands (eg. SB277011A, Figure 1).[1] However, known 6,7-dimethoxytetrahydroisoquioline σ2 ligands, like the known D3-preferring tetrahydroisoquinolines are flexible, extended molecules whereas the THPB scaffold is obviously a more rigid structure. To elucidate the importance of structural rigidity of the THPB core on σ2 and D3 receptor affinity, less rigid stepholidine analogues were prepared and evaluated. Given that THPBs have been known to show affinity for D1 and D2 receptors, the analogues were also assessed at D1 and D2 receptors to further gauge selectivity. Computational studies were also performed to help to rationalize observed affinities.

2.1 Chemistry

We engaged a route that we have recently reported for the synthesis of the THPB **10** for the synthesis of the C10 alkoxy derivatives.[35] This route is depicted in Scheme 1. Commercially available phenol **2** was reacted with ethoxymethyl chloride. The protected aryl bromide (**3**) thus formed was then treated with LDA (generated from reaction of *n*-BuLi with diisopropylamine) to afford diester **4**. Selective hydrolysis of the aliphatic ester in **4** gave acid **5**. Compound **5** was coupled to amine **6** and the resulting amide (**7**) was subjected to cyclization under Bischler-Napieralski conditions. Cyclization was accompanied by removal of the ethoxymethyl protecting group. The imine which formed was not isolated, but was treated thereafter with sodium borohydride, whereupon cyclization to afford the 8-oxoprotoberberine core ensued (compound **8**).

6

Reduction of the 8-oxo group of **8** with lithium aluminum hydride gave the THPB **9** containing the unprotected C10 phenol group. Williamson ether alkylation of phenol **9** with various alkyl halides afforded the C9 alkoxy/C2 benzyl protected derivatives. Finally, the benzyl group of these intermediates was removed by treatment with HCl in refluxing methanol to obtain the racemic C10 analogues **10**-**17**. Compound (±)-**1** was obtained by deprotection of the benzyl group of phenol **9** in similar fashion as for other C10 analogues.
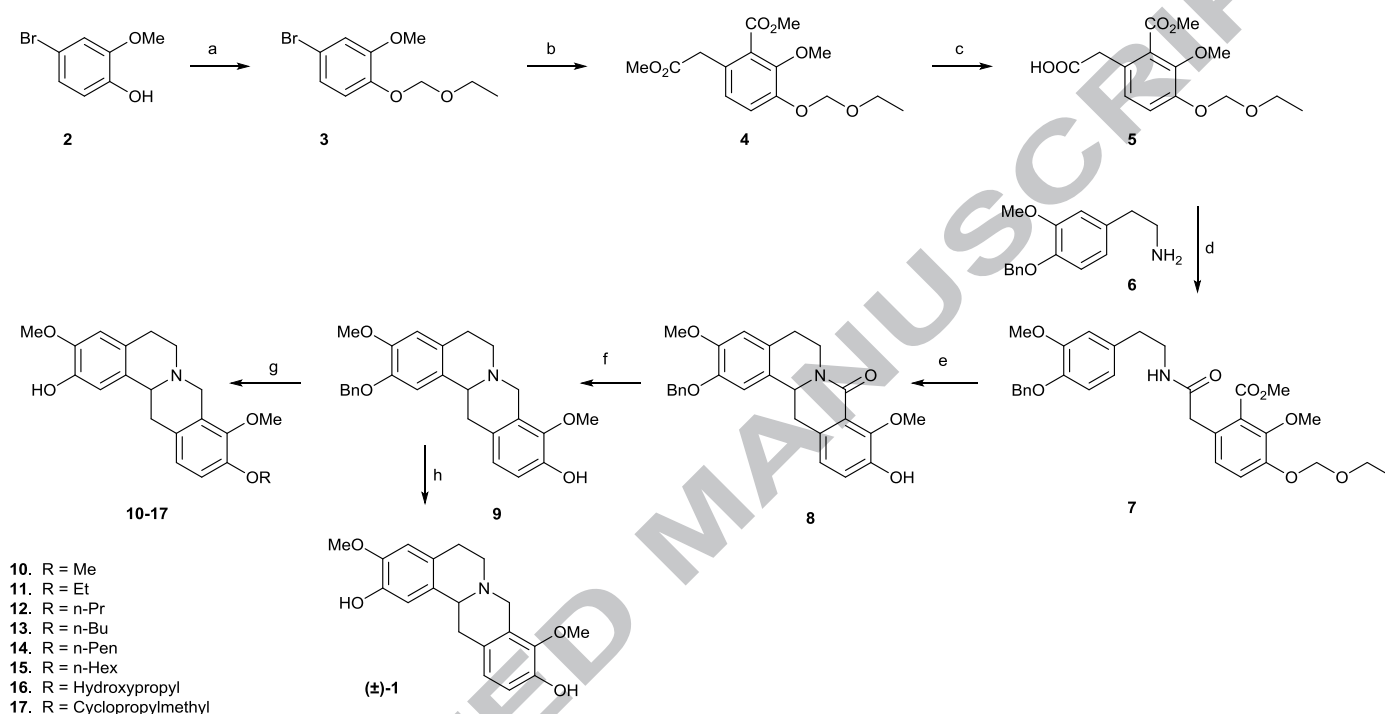
Scheme 1. Synthesis of C10 analogues. *Reagents and conditions*: (a) DIPEA, (chloromethoxy)ethane, DCM, 98%; (b) diisopropylamine, *n*-BuLi, DMM, THF, -78 °C, 54%; (c) K_2CO_3, 1:1 H_2O/MeOH, reflux, 95%; (d) CDI, THF, 78%; (e) i) $POCl_3$, CH_3CN, reflux; ii) $NaBH_4$, MeOH, 79% over 2 steps; (f) LAH, THF, reflux, 84%; (g) i) appropriate alkyl halide, DMF, CH_3CN, rt to reflux; ii) conc. HCl, MeOH, reflux; 64-77% over 2 steps; (h) conc. HCl, MeOH, reflux, 81 %

The route for preparation of the flexible analogues is shown in Scheme 2. Here, primary amine **6** was converted to the secondary amine **18** via reductive amination with 3-benzyloxy-2-methoxybezaldehyde. Pictet-Spengler cyclization followed by acidic debenzylation were implemented to convert **18** to the tetrahydroisoquinoline analogue **19**. A sequence of reductive amination and benzyl group hydrolysis reactions gave tertiary amines **20** and **21** from the secondary amine **18**.
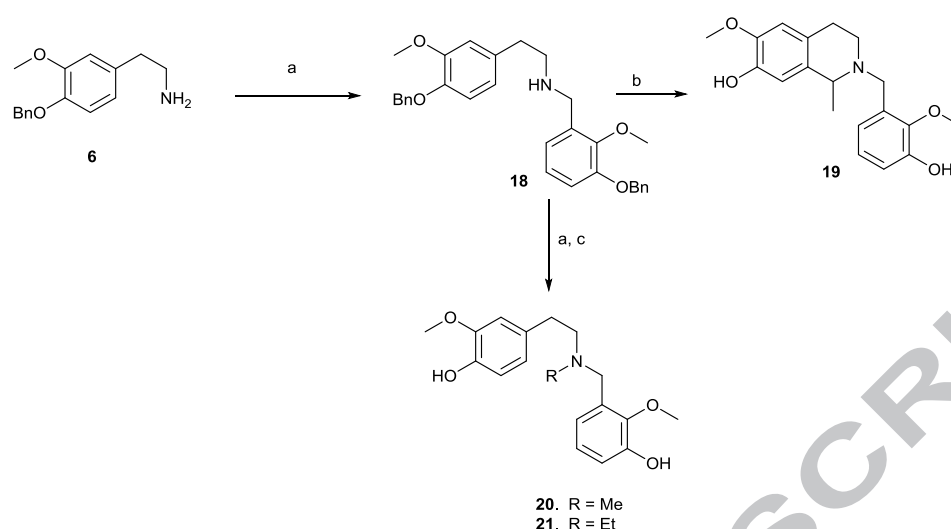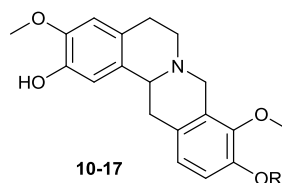
Scheme 2. Synthesis of flexible analogues. *Reagents and conditions*: a) Na(OAc)$_3$BH, DCM, rt, appropriate aldehyde; b) i) CF$_3$COOH, 1,1-diethoxyethane, DCM, rt; ii) Conc. HCl, MeOH, reflux, 60% over two steps; c) Conc. HCl, MeOH, reflux.

2.2 Biological evaluations

2.2.1 SAR on C10 analogues

Compounds (±)-**1**, **10-17** and **19-21** were assayed for binding affinity to human dopamine D1, D2 and D3 receptors and σ1 and σ2 receptors by the Psychoactive Drug Screening Program (PDSP). Details of the screening protocol may be found online at the PDSP website (https://pdspdb.unc.edu/pdspWeb/). In brief, the compounds were initially assayed in quadruplicate at a 10 μM concentration at D1, D2, D3, σ1 and σ2 receptors. Compounds that showed an inhibition of binding of >50% were progressed to secondary assays to measure K$_i$. The K$_i$ determinations were performed via 12-point concentration-response curves in triplicate (unless noted otherwise). This data is presented in Tables 1 (for C10 analogues) and 2 (for de-rigidified analogues).

(±)-**1** displayed approximately 20-fold stronger affinity for the D1 receptor as compared to the D2 and D3 receptors (K$_i$ of 5.6, 115.5 and 101 nM at D1, D2 and D3 respectively). For C10 alkoxy derivatives alkylation tends to reduce D1 affinity, with the analogues showing a 1.2 to 7-fold decrease in affinity as compared to (±)-**1**. The C10 phenol plays role but is not absolutely required for D1 affinity, given the relatively small drop in affinity seen for some analogues (for example **12** and **16**). This result is in accordance with observations from previous SAR work on the THPB framework by others.[32,31] Methyl and ethyl substituents resulted in an approximately 2-fold decrease in affinity (compounds **10** and **11** respectively). In the *n*-propyl (**12**) to *n*-hexyl (**15**) homologous series, a progressive decrease in affinity was observed. The D1 receptor affinity seen for the hydroxypropyl analogue **16** was comparable to that observed for (±)-**1** and the *n*-

Table 1. Affinity data (K_i in nM) for C10 analogues at dopamine and σ receptors

Compound	R	K_i (nM)[a]					Selectivity			
		D1[b]	D2[c]	D3[d]	σ1[e]	σ2[f]	D2/D1	D3/D1	D2/D3	σ1/σ2
(±)-1	H	5.6[g]	115.5[g]	101[g]	269	9.0	20.6	18.0	1.1	30
10	Me	15	102	37	106	1.0	6.8	2.5	2.8	106
11	Et	12.4	159	44	124	1.3	12.8	3.5	3.6	95
12	*n*-Pr	7.8	99	53	57	6.7	12.7	6.8	1.9	8.5
13	*n*-Bu	11	121	65	13	49	11	5.9	1.9	0.27
14	*n*-Pent	19	283	101	119	97	14.9	5.3	2.8	1.22
15	*n*-Hex	40	NA[h]	220	37	107	ND[i]	5.5	ND[i]	0.35
16	Hydroxypropyl	6.7	211	110	53	3.8	31.5	16.4	1.9	13.9
17	Cyclopropylmethyl	12	54	54	12	2.4	4.5	4.5	1	5

[a] Experiments carried out in triplicate - SEM values are within 13% of reported K_i; [b] [³H]SCH2390 used as radioligand/(+)-butaclamol used as reference compound - K_i = 2.3 nM; [c] [³H]N-methylspiperone used as radioligand/haloperidol used as reference compound - K_i = 9.6 nM; [d] [³H]N-methylspiperone used as radioligand/chlorpromazine used as reference compound - K_i = 11.0 nM; [e] [³H](+)-pentazocine used as radioligand/haloperidol used as reference compound - K_i = 1.1 nM; [f] [³H]DTG used as radioligand/haloperidol used as reference compound - K_i = 10.0 nM; [g] experiments carried out in duplicate; [h]NA- not active (<50% inhibition in primary assay therefore no secondary assay was performed); [i]ND - not determined

9

butyl analogue **13** (6.7, 5.6 and 11 nM respectively). This suggests that the hydroxyl group in **16** plays a relatively minor role in binding to the D1 receptor. The presence of the hydroxypropyl substituent in **16** restores the D1 affinity of stepholidine, improves the selectivity versus the D2 receptor (20.6 versus 31.5 for D2/D1 selectivity for stepholidine and **16** respectively) and retains the selectivity versus the D3 receptor (18 versus 16-fold for D3/D1 selectivity). Among the alkylated analogues, a 3 carbon chain length seems to be optimal for D1 affinity (consider **12** and **16**). The cyclopropylmethyl analogue (**17**) had similar affinity to the *n*-butyl analogue **13** and ethyl analogue **11**. Thus some degree of branching on the alkyl chain may be tolerated for D1 affinity.

On a whole, the D2 affinity of the analogues was lower than their D1 affinities. Thus the compounds retained selective affinity for the D1 receptor, as was observed in the lead molecule (±)-**1**. However, most compounds had lower than the 20-fold D1 selectivity seen for (±)-**1** (except for compounds **15** and **16**). Compounds in the homologous series from a methyl group to an *n*-butyl chain (**10**-**13**), had D2 affinities that are similar to (±)-**1,** ranging from 99 to 159 nM. However, compounds with the larger *n*-pentyl and *n*-hexyl chains had reduced affinities; in fact, the *n*-hexyl analogue (**15**) did not show any appreciable affinity for the D2 receptor (<50% inhibition) in the primary assay. The cyclopropylmethyl analogue (**17**) was the only compound in this series that displayed a significantly higher affinity for the D2 receptor than (±)-**1**.

There was a clear trend in the methyl to *n*-hexyl series at the D3 receptor, where an increase in the alkyl chain length was associated with a progressive decrease in affinity for the receptor. The hydroxypropyl analogue had similar affinity for the D3 receptor as compared to stepholidine. In the case of the cyclopropylmethyl analogue, D3 receptor affinity was improved two-fold as compared to stepholidine (54 nM vs 101 nM).

At the σ1 receptor, all analogues tested showed increased affinity as compared to (±)-**1** (ranging from approximately 2-fold to 22-fold increase in σ1affinity). Therefore, the C10 phenol functionality is not required for σ1 receptor affinity. No clear SAR trend could be discerned in the homologous series **10**-**15**. The *n*-butyl analogue **13** had the highest affinity of the compounds in this series [K_i = 13 nM for **13** vs 269 nM for (±)-**1**]. The hydroxypropyl analogue **16** had lower affinity than **13** (53 vs 13 nM) which suggests that the hydroxyl group in **16** does not have any significant binding interactions with the σ1 receptor (akin to observations at the D1 receptor). The cyclopropylmethyl and *n*-butyl analogues had similar σ1 affinities- approximately 12 nM (a situation that mirrors results for **17** at the D1 receptor). It thus appears that the cyclopropylmethyl group may function as a less hydrophobic bioisostere of the *n*-butyl group in this series at σ1 and D1 receptors.

A clear trend was seen at the σ2 receptor for analogues **10**-**15**, wherein there was a progressive decrease in σ2 receptor affinity as the alkyl chain was extended. Compounds **10** and **11** had the highest affinity of all compounds assayed (1 nM and 1.3 nM respectively), representing an approximately 7- to 9-fold higher σ2 receptor affinity than (±)-**1**. With respect to binding at σ receptors, both **10** and **11** exhibited higher σ2 receptor selectivity than compound (±)-**1** [approximately 100-fold for **10** and **11** versus 30-fold for compound
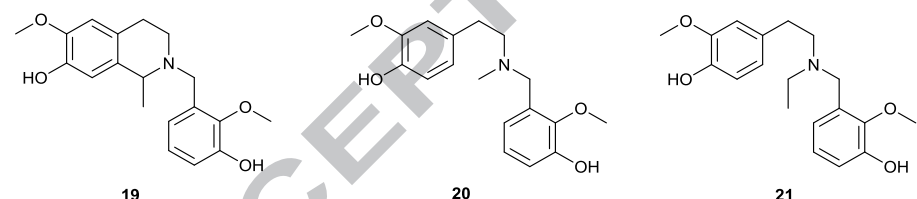
10

(±)-**1**]. All other analogues had decreased selective affinity for the σ2 receptor as compared to the σ1 receptor. In fact, this σ receptor selectivity was reversed for compounds **13** and **15** which both showed approximately 3-fold higher selectivity for σ1 versus σ2 receptors. Analogues **10**-**12** had higher affinity than (±)-**1**, indicating that small C10 alkoxy groups are better tolerated than the C10 phenolic group at the σ2 receptor. Compounds **16** and **17** displayed very high σ2 receptor affinity, comparable to **10** and **11;** thus there is some tolerance for small polar or hydrophobic groups at C10 for σ2 affinity.

2.2.2 SAR on flexible analogues

All de-rigidified analogues showed significantly lower affinity than (±)-**1** for dopamine D1, D2 and D3 receptors. Thus, the intact THPB core seems to be very important for affinity to dopamine receptors. Compounds **20** and **21** which lacked a tetrahydroisoquinoline motif had lower affinities for the D1, D2 and D3 receptor than compound **19** which possesses such a motif. Therefore it would appear that the presence of an intact tetrahydroisoquinoline moiety contributes significantly to dopamine receptor affinity.

De-rigidification did not significantly improve σ1 receptor affinity. Only a 2-fold increase in σ1 affinity was seen for compounds **19** and **20** as compared to (±)-**1**; a decrease in σ1 affinity was observed with compound **21**. All flexible analogues showed a deterioration in σ2 receptor affinity as compared to the lead (227 - 788 nM vs 9 nM). However, in general the de-rigidified analogues showed higher selectivity for σ receptors as compared to dopamine receptors suggesting that molecular flexibility is better tolerated at σ receptors within this series.

Table 2. K_i data for flexible analogues

Compound	D1[b]	D2[c]	D3[d]	σ1[e]	σ2[f]
			K_i (nM)[a]		
19	833	1095	1367	130	301
20	3111	>10,000	2680	122	227
21	>10000	>10000	1811	350	788

[a] Experiments carried out in triplicate - SEM values are within 13% of reported K_i; [b] [^{3}H]SCH2390 used as radioligand/(+)-butaclamol used as reference compound - K_i = 2.3 nM; [c] [^{3}H]N-methylspiperone used as radioligand/ haloperidol used as reference compound - K_i = 9.6 nM; [d] [^{3}H]N-methylspiperone used as radioligand/chlorpromazine used as reference compound - K_i = 11.0 nM; [e] [^{3}H](+)-pentazocine used as radioligand/ haloperidol used as reference compound - K_i = 1.1 nM; [f] [^{3}H]DTG used as radioligand/ haloperidol used as reference compound - K_i = 10.0 nM

2.2.3 Cytotoxicity evaluation

As alluded to before, some compounds have shown cytotoxic actions that are attributable to their interaction with σ receptors. We were curious to determine the extent to which our newly identified high affinity σ2 receptor ligands displayed cytotoxicity. Therefore, isocorypalmine (**10**), the most potent and selective σ2 ligand identified in this study, was selected for cytotoxicity evaluation in an Alamar Blue assay.[36] Compound **10** lacked significant cytotoxic activity in this assay, with an IC_{50} of 178 μM. Since σ2 receptor agonists are generally cytotoxic,[37-39] this result tends to imply that compound **10** is a σ2 receptor antagonist (although this needs to be ratified with further assays).

2.2.4 Receptor docking studies at the D3 receptor

The phenolic group at C10 of stepholidine does not seem to play a major role in its binding to dopamine D1 and D2 receptors (given the similarity in D1 and D2 affinities of the analogues as compared to stepholidine). In the case of the D3 receptor, a number of analogues had moderately improved affinity as compared to stepholidine. Therefore it seems that the C10 phenolic group is not an absolute necessity for affinity of stepholidine to the D3 receptor.

Table 3. Predicted binding affinity from Glidescore and ligand strain energy for C10 and flexible analogues at the D3 receptor prepared from the crystal structure with PDB code 3PBL

Compound	R	Glidescore	K_i at D3 (nM)
(±)-1	H	-7.9	101
10	Me	-7.5	37
11	Et	-7.4	44
12	n-Pr	-7.5	53
13	n-Bu	-7.4	65
14	n-Pent	-7.5	101
15	n-Hex	-7.3	220
16	Hydroxypropyl	-8.1	110
17	Cyclopropylmethyl	-7.3	54
19		-6.2	1367
20		-6.3	2680
21		-6.4	1811

Based on the SAR trend observed (increasing alkyl chain length decreases D3 affinity), it is apparent that the C10 alkoxy substituents of the analogues might project into a shallow hydrophobic pocket in the receptor. To get further clarity into this possibility, and to aid in rationalizing the D3 affinity trend observed, docking evaluations were performed on analogues **(±)-1**, **10-17** and **19-21** at the D3 receptor.

12
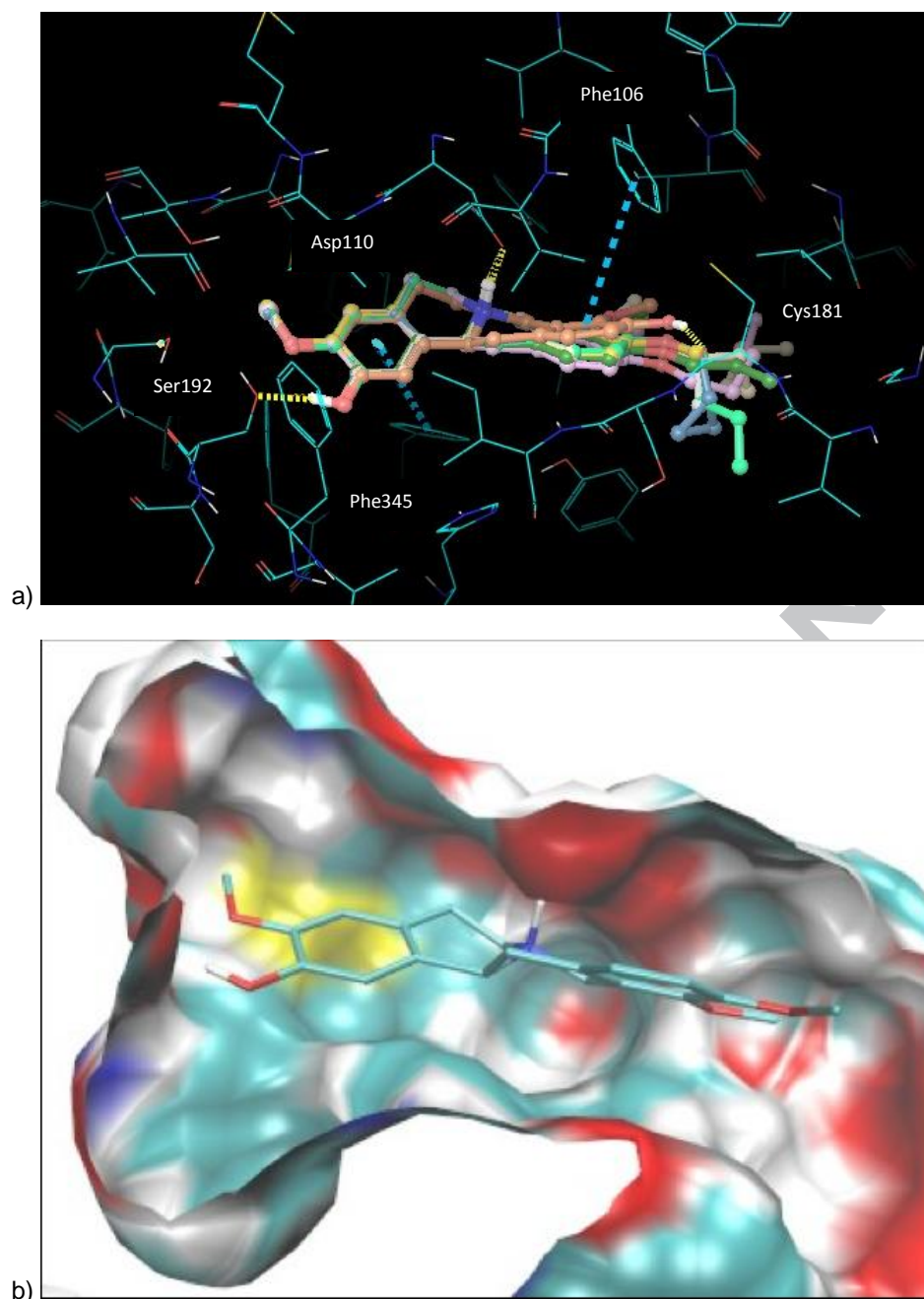
Figure 4. a) Docked poses of the lead molecule (±)-**1** and the C10 analogues **10**-**15** and **17**. Key hydrogen bonding interactions are given by the yellow dashed lines and hydrophobic interactions by the turquoise dashed lines. b) compound **10** docked in binding pocket

Investigation of the docked ligand poses and recognition of key protein-ligand interactions provides insights into the SAR outcomes of the series of C10 analogues and the de-rigidified compounds with respect to D3. In this study, ligand docking was performed retrospectively in order to elucidate and rationalize the measured D3 affinity data. Overall, the calculated binding energies for stepholidine and the C10 analogues are

13

in reasonable agreement with activities derived from the experimental data as shown in Table 3. Compounds **(±)-1**, **10-17** and **19-21** were docked into a pre-prepared 3-dimensional structure of the D3 receptor derived from the crystal structure with PDB code 3PBL.[34] A representation of the docked poses for the ligands **(±)-1**, **10-15** and **17** within the D3 receptor binding pocket is depicted in Figure 4. Each ligand generated multiple binding modes and the structures shown display the top ranked poses according to Glidescore (+ligand strain). These poses maintain key receptor-ligand interactions, including the critical protonated tertiary N – Asp110 salt bridge motif, H-bonds to Ser192 and Cys181 and hydrophobic interactions to Phe106 and Phe345 (Figure 4a). The analogues are positioned such that the aryl substituents project into hydrophobic cavities in the receptor (depicted in Figure 4b for compound **10**). The estimated binding energies according to Glidescore are very similar for this series of C10 analogue ligands, covering a narrow range from -7.9 to -7.3 kcal/mol. Overall, the relatively small decrease in the predicted binding energy as the length of the alkyl chain increases for compounds **10-15** qualitatively matches the decrease in the measured affinity for these ligands.
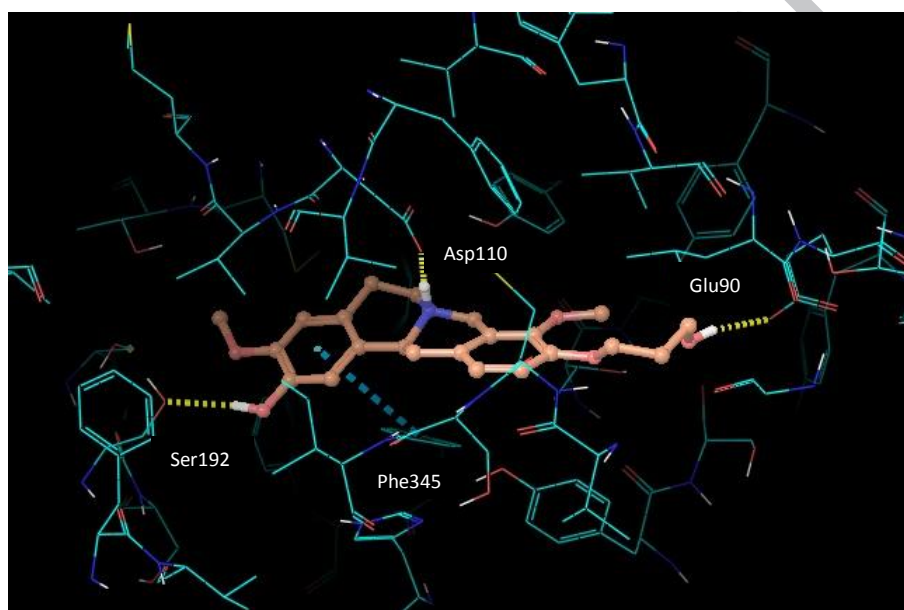
Figure 5. Docked pose of the hydroxypropyl analogue, compound **16**.

Quantitatively, the binding energy differences are very small compared to the wider, yet still relatively low, variation in measured affinities. The Glidescore value for stepholidine (-7.9 kcal/mol) was found to be lower than that for the other C10 analogues, including the cyclopropylmethyl analogue (-7.3 kcal/mol), in contrast to the experimental measurements. However, in a similar manner to the measured affinities, the hydroxypropyl analogue, with docked pose illustrated in Figure 5, had a predicted binding energy that is close to that of stepholidine (-8.1 kcal/mol vs -7.9 kcal/mol, respectively). Examination of the D3 receptor binding site shows that the alkyl, cyclopropylmethyl and hydroxypropyl groups of the C10 analogues fit into the extracellular hydrophobic region of the binding pocket, consisting of the extracellular loops and the junction of several

14

helices, without incurring any significant clashes with the protein structure. Hence, the small difference in predicted binding energies for these systems is unsurprising. The hydroxyl group in compound **16** also forms an additional H-bond to Glu90.

In agreement with the experimental affinity measurements at the D3 receptor, the de-rigidified, flexible compounds **19-21** are predicted to have significantly lower binding energies than the above more rigid C10 analogues according to the *in silico* docking outputs. The Glidescore values for the three compounds are very similar, ranging only from -6.4 kcal/mol to -6.2 kcal/mol. Analysis of the generated poses and the key protein-ligand interactions (depicted in Figures 6 and 7) suggests that the lowered affinity and predicted binding energy for these de-rigidified analogues is a consequence of (i) extra ligand flexibility, which leads to a small amount of strain for the ligand to fit in the site compared to the nearest minimized ligand conformation, and (ii) a lower lipophilic interaction score with the binding site residues due to lack of the tetrahydroisoquinoline motif (**20, 21**) and the THBP core (**19**). Each of these effects is relatively small (< 1 kcal/mol), however, the overall consequence is to reduce the binding affinity of the flexible analogues.
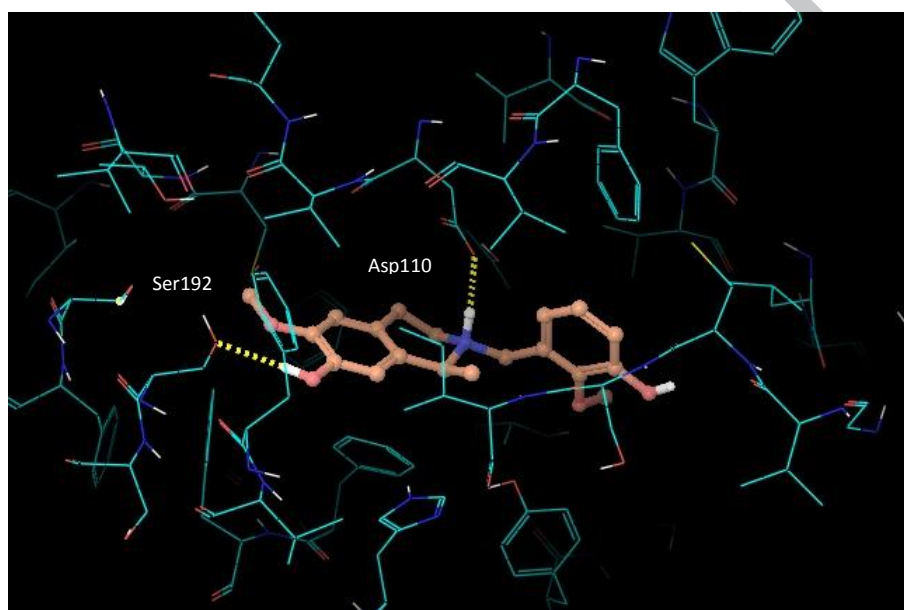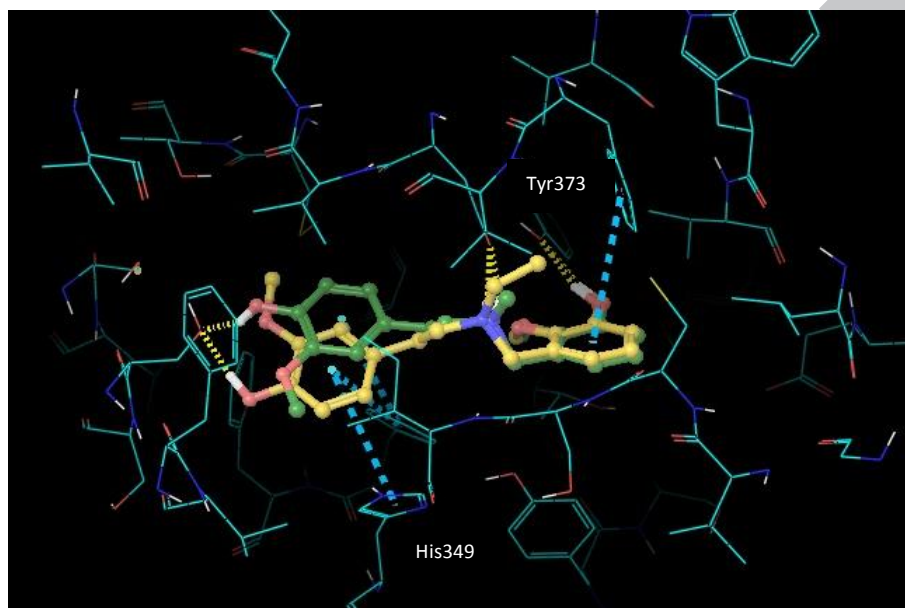

Figure 6. Docked pose of the flexible analogue, compound **19.**

Others have investigated docking of stepholidine at the D3 receptor computationally.[40] As compared to prior work, we found similarities in the key residues that are important for affinity of stepholidine (and the C10 analogues), particularly Asp110, Ser192 and Phe345. Apart from the key protonated nitrogen-Asp110 salt bridge interaction, in both studies Ser192 interacts with an aromatic hydroxyl group via a hydrogen bond and Phe345 interacts with an aromatic ring via aromatic stacking (Fig 4a). The main difference is that the orientation of stepholidine in our Glide docking study is reversed compared to the AutoDock derived pose in the previous work. Thus in our case Ser192 is H-bonded to the phenolic hydroxyl in ring A and Phe345 interacts with ring A, whereas in prior work Ser192 and Phe345 have interactions with the ring D hydroxyl and

ring D respectively. Given the close to symmetric structure of the molecule and its high rigidity, this reversal has little impact on the interactions with the receptor pocket, except for the formation of an additional H-bonding interaction between the phenolic group in ring D of stepholidine and the backbone O of Cys181 in our docked pose.

In order to assess the binding stability of flexible compounds **19-21** the ligands were simulated in complex with D3 (crystal structure 3pbl).[34] Ligand parameters were generated in Generalized Amber Force Field (GAFF),[41] protein parameters were assigned from AMBERFF14SB,[42] and the system was solvated in a 10 Å buffer of Tip4pew (~12000 water molecules). Ligands were allowed to move freely, however, protein heavy atoms were restrained with 2.5 kcal/Å^2 harmonic restraints to maintain model accuracy (in the absence of lipids). The starting configuration utilized for these simulations was the top ranked docked poses discussed above. These configurations were minimized and heated to 300 K, then equilibrated for 20 ns in NPT, and finally run in a 100 ns production NVT molecular dynamics simulation sampling every 1 ps.

Figure 7. Docked poses of the flexible analogues, compounds **20** and **21.**

The results of these simulations show that the docking poses are stable within this D3 configuration. Two metrics were utilized to assess ligand stability throughout the production simulations: ligand RMSD and the distance between the ligand's center of mass and Asp110 (critical for binding). Ligand RMSD was computed for each frame of the production trajectories compared to the ligand configuration in the original docked pose. This analysis shows that while ligand positions fluctuated over the course of the simulation, however, this did not differ greatly from their starting poses (Figure 8). The distance between ligand center of mass and Asp110 was utilized to determine whether the ligand maintained this key contact over the course of

the simulation. Though the distance does change by a small amount in compounds **19** and **21**, all three ligands maintain a bound state during the simulation (Figure 9). These data suggest that compounds **19-21** maintain a configuration similar to the predicted docked pose during a molecular dynamics simulation and that these predicted poses are stable with respect to the crystal D3 configuration. This supports the assertion that the difference in binding affinity is not likely due to destabilized binding, but rather the added ligand flexibility and decreased lipophilic interactivity.
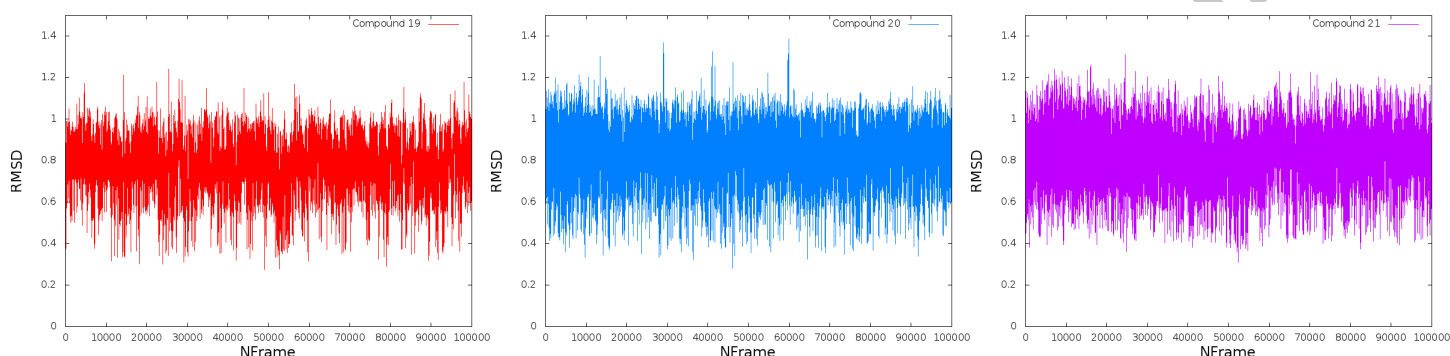
Figure 8. RMSD of flexible compounds **19** (left), **20** (middle) and **21** (right) between all atom coordinates at each frame, compared to the coordinates of the docked pose (starting configuration). All three compounds display limited motion within the binding site, fluctuating about their original docked pose.
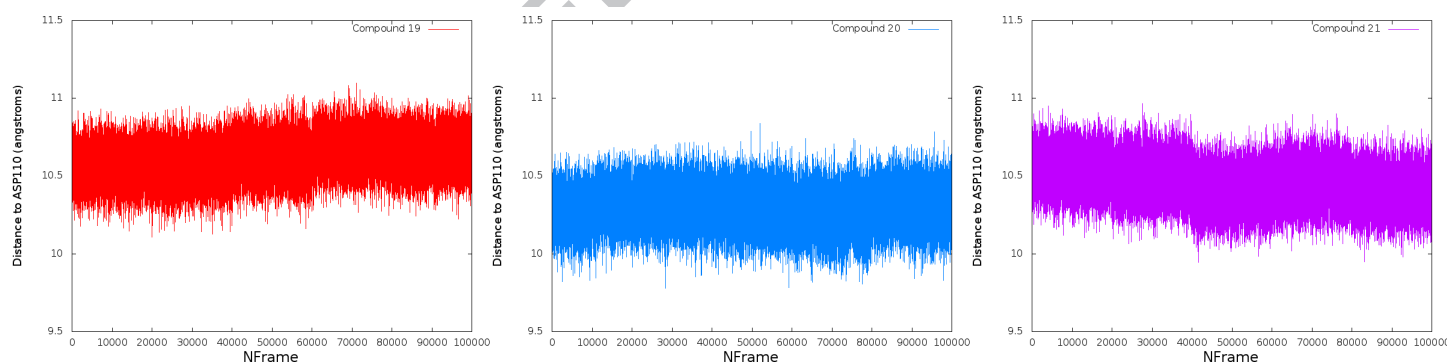
Figure 9. Distance between flexible compounds 19 (left), 20 (middle), and 21 (right) center of mass and the key aspartate Asp110 over the course of a 100 ns simulation. All three ligands maintain this contact throughout the sampled time.

3. Conclusions

The purpose of this study was to shed light on how substituent groups at the C10 position of THPBs as well as molecular rigidity impact σ2 receptor and D3 receptor affinity and selectivity (as compared to σ1, D1 and D2 receptors). Among the 5 receptors evaluated, the C10 THPB analogues seem to exhibit a general preference for the D1 receptor. The lowest D1 affinity seen for any analogue was 40 nM (for compound **15**).

17

Thus the C10 position seems to be fairly tolerant of alkoxy substituent groups with respect to D1 affinity. Of all C10 analogues tested, the lowest affinities were seen for D2 and σ1 receptors. Among the 3 dopamine receptors, affinity was generally highest for D1 receptor and lowest for the D2 receptor. Overall, the general order of affinities for C10 analogues at the 5 receptors evaluated is D1>σ-2>D3>D2≈σ1. However, individual compounds may exhibit high σ2 receptor affinity and selectivity. This is the situation with compounds **10** and **11**. Compound **10** is 15-fold more selective for the σ2 receptor as compared to the D1 receptor, thirty-seven-fold more selective as compared to the D3 receptor and approximately 100-fold more selective as compared to the σ1 receptor. A similar selectivity profile was obtained for compound **11**. The data suggests that relatively small *n*-alkoxy groups can be accommodated at C10 for high σ2 affinity *and* σ2 versus σ1 selectivity. It appears that high σ2 affinity may be obtained (perhaps to the detriment of selectivity) with small branched alkoxy groups (as is seen in for compound **17**). However the generality of this premise will be need to be tested via the evaluation of a larger set of analogues. Compound **10** is the racemic form of the known natural product isocorypalmine which has been reported to possess anti-cocaine effects in animals.[43] It is not clear at this time to what extent σ2 receptor affinity may play in this activity of naturally-occurring isocorypalmine. Rigidity of the THPB core seems to be important to impart high σ2 receptor affinity but de-ridification of the THPB core negatively impacts dopamine receptor affinity to a greater extent than σ receptor affinity.

The ligand binding energies from the D3 receptor docking studies show some similarities and minor discrepancies compared to the experimentally derived affinities. This is not surprising as empirical scoring functions, such as Glidescore used in this study, cannot rank order correctly and quantitatively discriminate all protein-ligand complexes based on the predicted scores. Such scoring functions work best in terms of distinguishing ligands as active or inactive, in contrast to quantitative rank ordering. In the current work, the relatively small series of compounds analyzed in the biological assays and *in silico* simulations, the relatively small range of affinities observed and the formation of multiple ligand binding modes in the D3 receptor binding pocket represent additional causes for the absence of a clear correlation between the docking outcomes and the experimentally derived affinities. Further exploration of a significantly larger and structurally more diverse ligand library would be required to provide deeper understanding and quantitative evaluation of the effectiveness of our *in silico* modeling process. Nevertheless, despite these issues, the predictive model successfully differentiated the flexible analogues from the more rigid systems and allowed for the identification of important protein-ligand interactions within the D3 receptor binding site that should potentially be conserved in the search for more active and selective compounds. The lack of crystal structures for σ receptors precluded similar studies at these receptors; this would have been similarly insightful, had it been possible.

This study is the first to investigate structural requirements of stepholidine analogues for affinity to σ receptors and the dopamine D3 receptor, via the utility of a combination of SAR and computational techniques. Our work has provided important revelations into the future design of THPB-based D3 and σ2 ligands and has uncovered compounds with higher D3 and σ2 receptor affinity than the lead, such as compound **10** and the

new THPBs **11, 12** and **17**. These compounds may be useful as leads for further SAR explorations to optimize σ2 and D3 affinity and selectivity. In closing, we posit that the THPB scaffold represents a good starting point from which to mine ligands with interesting mono- and multi-receptor profiles, particularly at dopamine D3 and σ2 receptors.

4. Experimental

4. 1   General methods

All moisture-sensitive and oxygen-sensitive reactions were carried out in flame-dried glassware under a nitrogen atmosphere. Solvents and all other reagents were purchased at the highest commercial quality from Aldrich and Fisher Scientific USA and used without further purification. Anhydrous sodium sulfate was used as drying agent for work-up of reactions. HRESIMS spectra were obtained using an Agilent 6520 QTOF instrument. ^{1}H NMR and ^{13}C NMR spectra were recorded using Bruker DPX-500 spectrometer (operating at 500 MHz for ^{1}H; 125 MHz, for ^{13}C) or Bruker Avance III spectrometer (operating at 400 MHz for ^{1}H; 100 MHz, for ^{13}C) using CDCl$_3$ as solvent, unless stated otherwise. Tetramethylsilane (δ 0.00 ppm) served as an internal standard in ^{1}H NMR and CDCl$_3$ (δ 77.0 ppm) in ^{13}C NMR unless stated otherwise. Chemical shift (δ 0.00 ppm) values are reported in parts per million and coupling constants in Hertz (Hz). Splitting patterns are described as singlet (s), doublet (d), triplet (t), and multiplet (m). Reactions were monitored by TLC with Whatman Flexible TLC silica gel G/UV 254 precoated plates (0.25 mm). TLC plates were visualized by UV (254 nm) and by staining in an iodine chamber. Flash column chromatography was performed with silica gel 60 (EMD Chemicals, 230-400 mesh, 0.063 µm particle size).

4.2   Chemistry

General procedure for synthesis of compounds 10-17 (as described for compound 10):

3,9,10-Trimethoxy-5,8,13,13a-tetrahydro-6*H*-isoquinolino[3,2-a]isoquinolin-2-ol (10)

Compound **9** (0.1 g, 0.24 mmol) was dissolved in DMF. Potassium carbonate (0.07 g, 0.48 mmol) and methyl iodide (0.02 mL, 0.36 mmol) were added and the reaction mixture was stirred overnight at rt. The crude reaction solution was filtered and the filtrate was evaporated to dryness. The residue was refluxed in a mixture of MeOH (5 mL) and concentrated HCl (3 mL) for 3 h. The MeOH was evaporated and the crude mixture was basified with ammonia solution, and extracted with DCM (3 × 15 mL). The combined organic layer was dried over anhydrous Na$_2$SO$_4$ and concentrated to give the crude product, which was purified by flash column chromatography on silica gel (2% MeOH/DCM) to give compound **10** (0.052 g, 64%) as an off-white solid; mp 208-210 °C; ^{1}H NMR (CDCl$_3$, 400 MHz) δ 6.87-6.77 (m, 3H), 6.60 (s, 1H), 5.56 (s, 1H), 4.24 (d, *J* = 15.7 Hz, 1H), 3.87 (s, 3H), 3.85 (s, 6H), 3.54-3.50 (m, 2H), 3.26-3.11 (m, 3H), 2.81 (dd, *J* = 16, 11.5 Hz, 1H), 2.68-2.61 (m, 2H); ^{13}C NMR (CDCl$_3$, 100 MHz) δ 150.2, 145.1, 143.9, 143.9, 130.6, 128.7, 127.9, 126.1, 124.0, 111.3,

111.0, 110.6, 60.2, 59.3, 59.3, 55.9, 54.0, 51.7, 36.3, 29.2; HRMS (ESI) *m/z* calcd. for $C_{20}H_{23}NO_4$ [M+H]$^+$, 342.1700, found 342.1704.

10-Ethoxy-3,9-dimethoxy-5,8,13,13a-tetrahydro-6*H*-isoquinolino[3,2-a]isoquinolin-2-ol (11)

Yield 67%; off-white powder, mp 186-188 °C ; ^{1}H NMR (CDCl$_3$, 400 MHz) δ 6.85-6.77 (m, 3H), 6.60 (s, 1H), 4.24 (d, *J* = 15.8 Hz, 1H), 4.06 (q, *J* = 7.0 Hz, 2H), 3.88 (s, 3H), 3.87 (s, 3H), 3.52 (d, *J* = 15.3 Hz, 2H), 3.27-3.10 (m, 3H), 2.84-2.61 (m, 3H), 1.44 (t, *J* = 7.0 Hz, 3H); ^{13}C NMR (CDCl$_3$, 100 MHz) δ 147.5, 143.5 143.2, 142.0, 128.7, 126.7, 125.9, 124.2, 122.0, 110.5, 109.5, 108.7, 62.5, 58.2, 57.4, 54.0, 52.2, 49.8, 34.4, 27.3, 13.1; HRMS (ESI) *m/z* calcd. for $C_{21}H_{25}NO_4$ [M+H]$^+$, 356.1856, found 356.1861.

3,9-Dimethoxy-10-propoxy-5,8,13,13a-tetrahydro-6*H*-isoquinolino[3,2-a]isoquinolin-2-ol (12)

Yield 68%; brown solid, mp 87-90 °C; ^{1}H NMR (CDCl$_3$, 500 MHz) δ 6.84-6.78 (m, 3H), 6.60 (s, 1H), 4.23 (d, *J* = 15.8 Hz, 1H), 3.94 (dt, *J* = 6.7, 1.8 Hz, 2H), 3.87 (s, 6H), 3.51 (d, *J* = 15.3 Hz, 2H), 3.25-3.10 (m, 3H), 2.80 (dd, *J* = 15.6, 11.4 Hz, 1H), 2.68-2.60 (m, 2H), 1.84 (sext, *J* = 7.1 Hz, 2H), 1.06 (t, *J* = 7.4 Hz, 3H); ^{13}C NMR (CDCl$_3$, 125 MHz) δ 149.6, 145.3, 145.1, 144.0, 130.6, 128.6, 127.8, 126.0, 123.8 112.3, 111.3, 110.6, 70.4, 60.2, 59.2, 55.9, 54.1, 51.7, 36.3, 29.2, 22.8, 10.7; HRMS (ESI) *m/z* calcd. for $C_{22}H_{27}NO_4$ [M+H]$^+$, 370.2013, found 370.2020.

10-Butoxy-3,9-dimethoxy-5,8,13,13a-tetrahydro-6*H*-isoquinolino[3,2-a]isoquinolin-2-ol (13)

Yield 73%; orange oil; ^{1}H NMR (CDCl$_3$, 400 MHz) δ 6.84-6.77 (m, 3H), 6.60 (s, 1H), 4.24 (d, *J* = 15.7 Hz, 1H) 3.98 (dt, *J* =1.0, 6.45 Hz, 2H), 3.86 (s, 6H), 3.52 (d *J* = 15.0 Hz, 2H), 3.25-3.10 (m, 3H), 2.80 (dd, *J* = 15.2, 11.3 Hz, 1H), 2.67-2.60 (m, 2H), 1.80 (quint, *J* = 6.9 Hz, 2H), 1.52 (sex, *J* = 7.6 Hz, 2H), 0.98 (t, *J* = 7.4 Hz, 3H); ^{13}C NMR (CDCl$_3$, 100 MHz) δ 149.6, 145.3, 145.1, 143.9, 130.5, 128.5, 127.7, 126.0, 123.8, 112.2, 111.3, 110.6, 68.5, 60.1, 59.2, 55.9, 54.0, 51.6, 36.2, 31.5, 29.2, 19.4, 13.9; HRMS (ESI) *m/z* calcd. for $C_{23}H_{29}NO_4$ [M+H]$^+$, 384.2169, found 384.2173.

3,9-Dimethoxy-10-(pentyloxy)-5,8,13,13a-tetrahydro-6*H*-isoquinolino[3,2-a]isoquinolin-2-ol (14)

Yield 65%; brown oil; ^{1}H NMR (CDCl$_3$, 400 MHz) δ 6.84-6.76 (m, 3H), 6.60 (s, 1H), 4.23 (d, *J* = 15.8 Hz, 1H), 3.97 (dt, *J* =1.5, 6.55 Hz, 2H), 3.87 (s, 6H), 3.51 (d, *J* = 15.2 Hz, 2H), 3.26-3.10 (m, 3H), 2.80 (dd, *J* = 15.7, 11.5 Hz, 1H), 2.68-2.60 (m, 2H), 1.82 (quint, *J* = 6.7 Hz, 2H), 1.49-1.36 (m, 4H), 0.93 (t, *J* = 7.2 Hz, 3H); ^{13}C NMR (CDCl$_3$, 100 MHz) δ 149.6, 145.3, 145.0, 143.9, 130.6, 128.6, 127.7, 126.1, 123.8, 112.3, 111.3, 110.6, 68.9, 60.2, 59.2, 55.9, 54.6, 51.6, 36.3, 29.2, 29.1, 28.3, 22.5, 14.0; HRMS (ESI) *m/z* calcd. for $C_{24}H_{31}NO_4$ [M+H]$^+$, 398.2326, found 398.2326.

10-(Hexyloxy)-3,9-dimethoxy-5,8,13,13a-tetrahydro-6*H*-isoquinolino[3,2-a]isoquinolin-2-ol (15)

Yield 70%; dark brown oil; ^{1}H NMR (CDCl$_3$, 500MHz) δ 6.84-6.76 (m, 3H), 6.60 (s, 1H), 4.23 (d, J = 15.7 Hz, 1H), 3.97 (t, J = 6.6 Hz , 2H), 3.86 (s, 6H), 3.53-3.50 (m, 2H), 3.26-3.10 (m, 3H), 2.80 (dd, J = 15.8, 11.6 Hz, 1H), 2.68-2.60 (m, 2H), 1.81 (quin, J = 6.7 Hz, 2H), 1.48 (quint, J= 7.2, 2H), 1.34 (sex, J = 3.8 Hz, 4H), 0.91 (t, J= 7.0 Hz, 3H); ^{13}C NMR (CDCl$_3$, 125 MHz) δ 149.6, 145.3, 145.0, 143.9, 130.6, 128.6, 127.7, 126.1, 123.8, 112.3, 111.4, 110.6, 68.9, 60.2, 59.2, 55.9, 54.1, 51.7, 36.3, 31.6, 29.4, 29.2, 25.8, 22.6, 14.0; HRMS (ESI) *m/z* calcd. for C$_{25}$H$_{33}$NO$_4$ [M+H]$^+$, 412.2482, found 412.2429.

10-(3-Hydroxypropoxy)-3,9-dimethoxy-5,8,13,13a-tetrahydro-6*H*-isoquinolino[3,2-a]isoquinolin-2-ol (16)

Yield 76%; reddish-brown solid, mp 73-78 °C; ^{1}H NMR (CDCl$_3$, 500MHz) 6.87-6.80 (m, 3H), 6.60 (s, 1H), 4.22 (d, J = 15.7 Hz, 1H), 4.16 (td, J = 6.1, 1.5 Hz, 2H), 3.91-3.84 (m, 8H), 3.52 (d, J = 15.4 Hz, 2H), 3.27-3.10 (m, 3H), 2.80 (dd, J = 15.7, 11.6 Hz, 1H), 2.68-2.61 (m, 2H), 2.07 (quint, J = 5.8 Hz, 2H); ^{13}C NMR (CDCl$_3$, 125 MHz) δ 149.4, 145.4, 145.1, 143.9, 130.5, 128.8, 128.4, 126.1, 124.1, 112.5, 111.3, 110.6, 67.5, 61.0, 60.3, 59.2, 55.9, 54.0, 51.6, 36.3, 32.1, 29.2; HRMS (ESI) *m/z* calcd. for C$_{22}$H$_{27}$NO$_5$ [M+H]$^+$, 386.1884, found 386.1897.

10-(Cyclopropylmethoxy)-3,9-dimethoxy-5,8,13,13a-tetrahydro-6*H*-isoquinolino[3,2-a]isoquinolin-2-ol (17)

Yield 81%; yellow oil; ^{1}H NMR (CDCl$_3$, 500 MHz) δ 6.83-6.76 (m,3H), 6.60 (s, 1H), 4.23 (d, J = 15.7 Hz, 1H), 3.90- 3.83 (m, 8H), 3.51 (d, J = 15.1 Hz, 2H), 3.26-3.11 (m, 3H), 2.80 (dd, J = 15.0, 12.0 Hz, 1H), 2.68-2.62 (m, 2H), 1.31-1.27 (m, 1H), 0.61 (q, J = 5.7 Hz, 2H), 0.36 (q, J = 4.85 Hz, 2H); ^{13}C NMR (CDCl$_3$, 125 MHz) δ 149.5, 145.7, 145.0, 143.9, 130.6, 128.6, 128.1, 126.1, 123.8, 113.1, 111.3, 110.6, 73.9, 60.2, 59.2, 55.9, 54.1, 51.6, 36.3, 29.2, 10.5, 3.2, 3.2; HRMS (ESI) *m/z* calcd. for C$_{23}$H$_{27}$NO$_4$ [M+H]$^+$, 382.2013, found 382.2019.

N-(3-(Benzyloxy)-2-methoxybenzyl)-2-(4-(benzyloxy)-3-methoxyphenyl)ethan-1-amine (18)

Amine **6** (0.25g, 0.97 mmol) and 3-(benzyloxy)-2-methoxybenzaldehyde (0.24 g ,0.97 mmol) were dissolved in DCM and the solution stirred at 0 ºC for 10 min. Sodium triacetoxyborohydride (0.31 g, 1.5 mmol) was added to the reaction mixture at 0 ºC and allowed to stir for 3 h at rt. The reaction mixture was washed with saturated NaHCO$_3$ and the organic layer was dried over sodium sulfate and concentrated to give the compound **18** (0.4 g, 83%) as a brown oil; ^{1}H NMR (CDCl$_3$, 500MHz) δ 7.40-7.27 (m, 10H), 6.98-6.95 (m, 1H), 6.89-6.6.85 (m, 2H), 6.79-6.74 (m, 2H), 6.66 (dd, J = 1.6, 8.1 Hz, 1H), 5.12 (s, 2H), 5.10 (s, 2H), 3.85-3.79 (m, 8H), 2.86 (t, J = 7.3, 2H), 2.77 (t, J = 7.3 Hz, 2H); ^{13}C NMR (CDCl$_3$, 125 MHz) δ 151.6, 149.5, 147.7, 146.5, 137.3, 137.0, 133.5, 133.0, 128.6, 128.5, 128.0, 127.7, 127.3, 127.2, 123.8, 122.2, 122.1, 121.3, 120.6, 114.7, 114.1, 113.3, 112.4, 111.9, 71.1, 70.1, 60.7, 55.9, 50.3, 48.8, 35.7 ; HRMS (ESI) *m/z* calcd. for C$_{31}$H$_{33}$NO$_4$ [M+H]$^+$, 484.2488, found 484.2475.

2-(3-Hydroxy-2-methoxybenzyl)-6-methoxy-1-methyl-1,2,3,4-tetrahydroisoquinolin-7-ol (19)

Compound **18** (0.3 g, 0.6 mmol) was dissolved in DCM. 1,1 diethoxyethane (0.13 mL, 0.9 mmol) and TFA (0.14 mL, 1.8 mmol) were added to the reaction mixture and allowed to stir o.n. The reaction mixture was washed with saturated $NaHCO_3$ and organic layer was dried over sodium sulfate and evaporated to dryness. The residues were refluxed in a mixture of MeOH (5 mL) and concentrated HCl (3 mL) for 3 h. The methanol was evaporated and the crude mixture was basified with ammonia solution, and extracted with dichloromethane (3 × 10 mL). The combined organic layer was dried over sodium sulfate and concentrated to give the crude product, which was purified by flash column chromatography on silica gel (3% MeOH/DCM)   to give the compound **19** (0.12 g, 60%) as a yellow powder, mp 56-58 °C; ^1H NMR (CDCl$_3$, 500 MHz) δ 7.00-6.98 (m, 2H), 6.88 (dd, J =6.85, 2.8 Hz, 1H), 6.64 (s, 1H), 6.55 (s, 1H), 3.85-3.79 (m, 8H), 3.67 (d, J = 13.6 Hz, 1H), 3.07-3.02 (m, 1H), 2.83-2.77 (m, 1H), 2.68 (dt, J = 12.5, 4.5 Hz, 1H), 2.58 (dt, J = 13, 4.5 Hz, 1H), 1.37 (d, J = 6.6 Hz, 3H); ^{13}C NMR (CDCl$_3$, 125 MHz) δ 149.0, 145.9, 144.9, 143.6, 133.0, 132.7, 125.6, 124.6, 122.1, 114.3, 113.0, 110.6, 61.8, 56.3, 55.9, 52.2, 44.0, 27.0, 20.0; HRMS (ESI) *m/z* calcd. for C$_{19}$H$_{23}$NO$_4$ [M+H]$^+$, 330.1700, found 330.1707.

General procedures for synthesis of compounds 20 and 21 (as described for compound 20):

3-(((4-Hydroxy-3-methoxyphenethyl)(methyl)amino)methyl)-2-methoxyphenol (20)

Amine **18** (0.2g, 0.41 mmol) and formaldehyde (0.06 mL, 1.64 mmol) were dissolved in DCM and allowed to stir the solution at 0 ºC for 10 minutes. Sodium triacetoxy borohydride (0.13g, 0.62 mmol) was added in to the reaction mixture at 0 ºC and allowed it to stir for 3 h at room temperature. Reaction mixture was washed with saturated $NaHCO_3$ and organic layer was dried over sodium sulfate and concentrated. The residues were refluxed in to the mixture of methanol (5 mL) and concentrated HCl (3 mL) for 3 h. Methanol was evaporated and the crude mixture was basified with ammonia solution, and extracted with dichloromethane (10 mL × 3). The combined organic layers were dried over sodium sulfate and concentrated to give the crude product, which was purified by flash column chromatography on silica gel (3% methanol/dichloromethane)   to give the compound **20** (0.1g, 74%) as a yellow oil; ^1H NMR (CDCl$_3$, 500 MHz) δ 7.0-6.89 (m, 3H), 6.82 (d, J = 8.1 Hz, 1H), 6.68-6.66 (m, 2H), 3.86 (s, 3H), 3.80 (s, 3H), 3.64 (s, 2H), 2.79 (s, 2H), 2.70 (s, 2H), 2.33 (s, 3H); ^{13}C NMR (CDCl$_3$, 125 MHz) δ 149.0, 146.3, 145.9, 143.8, 124.7, 122.5, 121.2, 121.2, 114.2, 114.1, 114.0, 111.2, 61.7, 55.9, 55.7, 52.2, 42.0, 33.3; HRMS (ESI) *m/z* calcd. for C$_{18}$H$_{23}$NO$_4$ [M+H]$^+$, 318.1700, found 318.1693

3-((Ethyl(4-hydroxy-3-methoxyphenethyl)amino)methyl)-2-methoxyphenol (21)

Yield 68%, brown oil; ^1H NMR (CDCl$_3$, 500MHz) δ 6.98-6.93 (m, 2H), 6.87 (dd, J = 2.0, 7.5 Hz, 1H), 6.80 (d, J = 8.4 Hz, 1H), 6.65-6.64 (m, 2H), 3.85 (s, 3H), 3.80 (s, 3H), 3.67 (s, 2H), 2.71 (s, 4H), 2.62 (q, J = 6.8 Hz, 2H), 1.1 (t, J = 7.0 Hz, 3H); ^{13}C NMR (CDCl$_3$, 125 MHz) δ 149.0, 146.3, 145.7, 143.7, 124.6, 122.3, 121.3, 121.3,

114.3, 114.1, 114.1, 111.2, 61.7, 55.8, 55.3, 51.9, 47.5, 33.0, 11.8; HRMS (ESI) *m/z* calcd. for $C_{19}H_{25}NO_4$ $[M+H]^+$, 332.1856, found 332.1851.

References

1. Micheli, F.; Heidbreder, C. *Expert Opin. Ther. Pat* .**2013,** *23*, 363.
2. Heidbreder, C. *CNS Neurol. Disord. Drug Targets* **2008,** *7*, 410.
3. Keck, T. M.; John, W. S.; Czoty, P. W.; Nader, M. A.; Newman, A. H. *J Med Chem* **2015,** *58*, 5361.
4. Heidbreder, C. *Naunyn Schmiedebergs Arch. Pharmacol.* **2013,** *386*, 167.
5. Luedtke, R. R.; Rangel-Barajas, C.; Malik, M.; Reichert, D. E.; Mach, R. H. *Curr. Pharm. Des.* **2015,** *21*, 3700
6. Pich, E. M.; Collo, G. *Eur Neuropsychopharmacol.* **2015,** *25*, 1437.
7. Gross, G.; Wicke, K.; Drescher, K. U. *Naunyn Schmiedebergs Arch. Pharmacol.* **2013,** *386*, 155.
8. Hackling, A. E.; Stark, H. *Chembiochem* **2002,** *3*, 946.
9. Newman, A. H.; Grundt, P.; Nader, M. A. *J. Med. Chem.* **2005,** *48*, 3663.
10. Bouchard, P.; Quirion, R. *Neuroscience* **1997,** *76*, 467.
11. Quirion, R.; Bowen, W. D.; Itzhak, Y.; Junien, J. L.; Musacchio, J. M.; Rothman, R. B.; Su, T. P.; Tam, S. W.; Taylor, D. P. *Trends Pharmacol. Sci.* **1992,** *13*, 85.
12. McCann, D. J.; Weissman, A. D.; Su, T. P. *Synapse* **1994,** *17*, 182.
13. Hellewell, S. B.; Bruce, A.; Feinstein, G.; Orringer, J.; Williams, W.; Bowen, W. D. *Eur. J. Pharmacol.* **1994,** *268*, 9.
14. McCann, D. J.; Su, T. P. *Eur. J. Pharmacol.* **1990,** *188*, 211.
15. Guitart, X.; Codony, X.; Monroy, X. *Psychopharmacology (Berl)* **2004,** *174*, 301.
16. Walker, J. M.; Bowen, W. D.; Walker, F. O.; Matsumoto, R. R.; De Costa, B.; Rice, K. C. *Pharmacol. Rev.* **1990,** *42*, 355.
17. Matsumoto, R. R.; Nguyen, L.; Kaushal, N.; Robson, M. J. *Adv. Pharmacol.* **2014,** *69*, 323.
18. Robson, M. J.; Noorbakhsh, B.; Seminerio, M. J.; Matsumoto, R. R. *Curr. Pharm. Des.* **2012,** *18*, 902.
19. Fishback, J. A.; Robson, M. J.; Xu, Y. T.; Matsumoto, R. R. *Pharmacol. Ther.* **2010,** *127*, 271.
20. Matsumoto, R. R. *Expert Rev. Clin. Pharmacol.* **2009,** *2*, 351.
21. Abate, C.; Niso, M.; Infantino, V.; Menga, A.; Berardi, F. *Eur. J. Pharmacol.* **2015,** *758*, 16.
22. Zeng, C.; Garg, N.; Mach, R. H. *Mol. Imaging Biol.* **2015**.
23. Xu, J.; Zeng, C.; Chu, W.; Pan, F.; Rothfuss, J. M.; Zhang, F.; Tu, Z.; Zhou, D.; Zeng, D.; Vangveravong, S.; Johnston, F.; Spitzer, D.; Chang, K. C.; Hotchkiss, R. S.; Hawkins, W. G.; Wheeler, K. T.; Mach, R. H. *Nat. Commun.* **2011,** *2*, 380.
24. Mach, R. H.; Smith, C. R.; al-Nabulsi, I.; Whirrett, B. R.; Childers, S. R.; Wheeler, K. T. *Cancer Res.* **1997,** *57*, 156.

25. Wheeler, K. T.; Wang, L. M.; Wallen, C. A.; Childers, S. R.; Cline, J. M.; Keng, P. C.; Mach, R. H. *Br. J. Cancer* **2000,** *82*, 1223.
26. Zeng, C.; Rothfuss, J.; Zhang, J.; Chu, W.; Vangveravong, S.; Tu, Z.; Pan, F.; Chang, K. C.; Hotchkiss, R.; Mach, R. H. *Br. J. Cancer* **2012,** *106*, 693.
27. van Waarde, A.; Rybczynska, A. A.; Ramakrishnan, N. K.; Ishiwata, K.; Elsinga, P. H.; Dierckx, R. A. *Biochim. Biophys. Acta.* **2015,** *1848*, 2703.
28. Mach, R. H.; Zeng, C.; Hawkins, W. G. *J. Med. Chem.* **2013,** *56,* 7137.
29. Hornick, J. R.; Spitzer, D.; Goedegebuure, P.; Mach, R. H.; Hawkins, W. G. *Surgery* **2012,** *152*, S152.
30. Makvandi, M.; Tilahun, E. D.; Lieberman, B. P.; Anderson, R. C.; Zeng, C.; Xu, K.; Hou, C.; McDonald, E. S.; Pryma, D. A.; Mach, R. H. *Biochem. Biophys. Res. Commun.* **2015,** *467*, 1070.
31. Sun, H.; Zhu, L.; Yang, H.; Qian, W.; Guo, L.; Zhou, S.; Gao, B.; Li, Z.; Zhou, Y.; Jiang, H.; Chen, K.; Zhen, X.; Liu, H. *Bioorg. Med. Chem.* **2013,** *21*, 856.
32. Qian, W.; Lu, W.; Sun, H.; Li, Z.; Zhu, L.; Zhao, R.; Zhang, L.; Zhou, S.; Zhou, Y.; Jiang, H.; Zhen, X.; Liu, H. *Bioorg. Med. Chem.* **2012,** *20*, 4862.
33. Roth, B. L.; Lopez, E.; Beischel, S.; Westkaemper, R. B.; Evans, J. M. *Pharmacol. Ther.* **2004,** *102*, 99.
34. Chien, E. Y.; Liu, W.; Zhao, Q.; Katritch, V.; Han, G. W.; Hanson, M. A.; Shi, L.; Newman, A. H.; Javitch, J. A.; Cherezov, V.; Stevens, R. C. *Science* **2010,** *330*, 1091.
35. Gadhiya, S.; Ponnala, S.; Harding, W. W. *Tetrahedron* **2015,** *71*, 1227.
36. Nakayama, G. R.; Caton, M. C.; Nova, M. P.; Parandoosh, Z. *J. Immunol. Methods* **1997,** *204*, 205.
37. Behensky, A. A.; Yasny, I. E.; Shuster, A. M.; Seredenin, S. B.; Petrov, A. V.; Cuevas, J. *J. Pharmacol. Exp. Ther.* **2013,** *347*, 458.
38. Rybczynska, A. A.; Dierckx, R. A.; Ishiwata, K.; Elsinga, P. H.; van Waarde, A. *J. Nucl. Med.* **2008,** *49*, 2049.
39. Korpis, K.; Weber, F.; Wunsch, B.; Bednarski, P. J. *Pharmazie* **2014,** *69*, 917.
40. Li, B.; Li, W.; Du, P.; Yu, K. Q.; Fu, W. *J. Phys. Chem. B* **2012,** *116*, 8121.
41. Wang, J.; Wolf, R. M.; Caldwell, J. W.; Kollman, P. A.; Case, D. A. *J. Comput. Chem.* **2004,** *25*, 1157.
42. Maier, J. A.; Martinez, C.; Kasavajhala, K.; Wickstrom, L.; Hauser, K. E.; Simmerling, C. *J. Chem. Theory Comput.* **2015,** *11*, 3696.
43. Xu, W.; Wang, Y.; Ma, Z.; Chiu, Y. T.; Huang, P.; Rasakham, K.; Unterwald, E.; Lee, D. Y.; Liu-Chen, L. Y. *Drug Alcohol Depend.* **2013,** *133,* 693.